

1 **Gold Nanoparticles Disturb Small Extracellular Vesicle Attributes of**  
2 **Mouse Embryonic Stem Cells**

3 Fang Hao,<sup>†,‡</sup> Tingting Ku,<sup>§</sup> Xiaoxi Yang,<sup>†</sup> Qian S. Liu,<sup>†</sup> Xingchen Zhao,<sup>†</sup> Francesco  
4 Faiola,<sup>†,‡</sup> Qunfang Zhou,<sup>\*,†,‡,‡,‡</sup> Guibin Jiang<sup>†,‡,‡</sup>

5  
6 <sup>†</sup>State Key Laboratory of Environmental Chemistry and Ecotoxicology, Research  
7 Center for Eco-Environmental Sciences, Chinese Academy of Sciences, Beijing  
8 100085, China

9 <sup>‡</sup>College of Resources and Environment, University of Chinese Academy of Sciences,  
10 Beijing 100049, China

11 <sup>§</sup>College of Environment and Resource, Research Center of Environment and Health,  
12 Shanxi University, Taiyuan, 030006, China

13 <sup>‡</sup>School of Environment, Hangzhou Institute for Advanced Study, University of  
14 Chinese Academy of Sciences, Hangzhou, 310000, China

15

16

17

18

19

20

21

22

23

24 \* Correspondence to:

25 Dr. Qunfang Zhou, State Key Laboratory of Environmental Chemistry and  
26 Ecotoxicology, Research Center for Eco-Environmental Sciences, Chinese Academy  
27 of Sciences, Beijing 100085, China.

28 E-mail: zhouqf@rcees.ac.cn

29

## 30 **Materials and methods**

31 **Reagents.** The aqueous solutions (1 mg/mL) of three kinds of AuNPs (AuNP-5,  
32 AuNP-20, and AuNP-80) were purchased from Nanocomposix Company (USA), and  
33 their surfaces were all functionalized with citrate sodium coatings. The stock solution  
34 was sonicated and diluted with cell culture medium to prepare the corresponding  
35 working solution. All the other chemicals were bought from Sigma-Aldrich, unless  
36 specifically stated otherwise.

37 **AuNP characterization.** The aqueous solutions of AuNP-5, AuNP-20, and AuNP-80  
38 (50  $\mu\text{g/mL}$ , 2  $\mu\text{L}$ ) were dropped onto the carbon film-coated grids and dried at room  
39 temperature. The as-prepared samples were observed and photographed using a  
40 transmission electronic microscope (TEM, JEOL H7500, Japan) at the accelerating  
41 voltage of 200 kV. Localized surface plasmon resonance absorption spectra ranging  
42 from 400 nm - 800 nm were obtained for the test AuNPs using quartz cells on a NIR-  
43 3600 spectrometer (Shimadzu, Japan). Their hydrodynamic sizes and zeta potentials  
44 were analyzed by a Malvern Zetasizer Nano ZS (Malvern, UK), and the measurement  
45 of each sample was replicated for three times. Hyperspectra microscopy (Cytoviva  
46 Inc., USA) was used to get the enhanced dark-field images of AuNPs under oil  
47 immersion objective (63 $\times$ ) for further hyperspectral analysis.

48 **Culture of mouse embryonic stem cells (mESCs).** The J1 mESCs (Shanghai  
49 Institute of Biochemistry and Cell Biology, Chinese Academy of Sciences) were  
50 seeded in 6-well plates pre-coated with 0.1% gelatin (Merck Millipore, USA), and  
51 cultured in KSR medium, which was KnockOut DMEM (Gibco, USA) supplemented  
52 with 15% serum replacement (Gibco, USA), 1% Glutamax-I, 1% MEM non-essential  
53 amino acids, 1% penicillin and streptomycin (Gibco, USA),  $5\times 10^{-5}$  mol/L  $\beta$ -  
54 mercaptoethanol (Solarbio, China), and 1% leukemia inhibitory factor (LIF,  $1\times 10^7$   
55 U/mL, Merck Millipore, Germany) at 37  $^{\circ}\text{C}$  and 5%  $\text{CO}_2$  for 12 h. Then, the mESCs  
56 were cultured in the complete N2B27 medium, according to previously reported  
57 protocol for another 48 h.<sup>1</sup> All exposure experiments of AuNPs were started when

58 N2B27 medium was introduced.

59 **Cell viability assay.** The cell viability experiment was firstly performed to screen the  
60 non-cytotoxic concentrations of the test AuNPs (i.e. AuNP-5, AuNP-20, and AuNP-  
61 80). Briefly, the mESCs were seeded in 0.1% gelatin pre-coated 96-well plates at the  
62 density of 10,000 cells per well and cultured in KSR medium. After 24 h, the medium  
63 was replaced with fresh N2B27 medium containing a series of concentrations of  
64 AuNPs (0, 0.1, 0.5, 1, 5, 10, 25, 50, 75, 100  $\mu\text{g}/\text{mL}$ ) and cultured for 24 h and 48 h,  
65 respectively. After exposure, the cells were incubated with 10  $\mu\text{M}$  resazurin reagent  
66 for another 2 h at 37  $^{\circ}\text{C}$ . The fluorescence at 530 nm/590 nm ( $\lambda_{\text{excitation}}/\lambda_{\text{emission}}$ )  
67 was recorded by a multiplate reader (VARIOSKAN FLASH, Thermo Fisher  
68 Scientific, USA). The fluorescence intensities of exposure groups relative to that of  
69 the negative control were finally evaluated.

70 **Measurement of reactive oxygen species (ROS) in mESCs.** A commercially  
71 available kit (Beyotime, China) was used for the measurement of ROS generation in  
72 mESCs upon AuNP treatments. Briefly, the mESCs incubated in 96-well plates were  
73 firstly loaded with 10  $\mu\text{M}$  non-fluorescent probe (DCFH-DA) in N2B27 medium.  
74 Thirty minutes later, 1  $\mu\text{g}/\text{mL}$  AuNPs (i.e. AuNP-5, AuNP-20, and AuNP-80) were  
75 added and the exposure lasted for 1 h, 6 h and 24 h, respectively. The fluorescence at  
76  $\lambda_{\text{excitation}}/\lambda_{\text{emission}}$  of 485 nm/530 nm was measured on a multiplate reader  
77 (VARIOSKAN FLASH, Thermo Fisher Scientific, USA). The positive control was  
78 set by using 1-h exposure of 10 mM  $\text{H}_2\text{O}_2$ , and the negative control was the mESCs  
79 without AuNP treatments. The final results were expressed by the fluorescence  
80 intensities of exposure groups relative to that of the negative control.

81 **Hyperspectral microscopic observation.** The mESCs were seeded on the glass-slip  
82 (CITOGLAS, China) pre-coated by 0.1 % gelatin, and cultured in KSR medium for  
83 24 h. The cells were then submitted to subsequent 48-h culture in N2B27 medium  
84 with or without 1  $\mu\text{g}/\text{mL}$  AuNPs (i.e. AuNP-5, AuNP-20, and AuNP-80). After  
85 treatment, the mESCs were washed by PBS for 3 times and fixed in 4%  
86 paraformaldehyde (PFA) for 20 min. After 3-time wash, the cell specimens were

87 sealed on the glass-slip with nail polish. The as-prepared slides were observed and  
88 imaged under the enhanced dark field hyperspectral microscope equipped with a  
89 spectrograph CCD camera (Cytoviva Inc., USA). The hyperspectral spectrum from  
90 400 nm to 900 nm with the exposure time of 0.1 s was obtained for at least 30  
91 nanoparticles in each sample. The final acquisition and analyses were conducted using  
92 ENVI software (version 4.8. Harris Corporation, USA).

93 **Elemental analysis of Au in mESCs.** The mESCs seeded in 6-well plates at the  
94 density of  $1 \times 10^5$  cells per well were exposed to  $1 \mu\text{g/mL}$  AuNPs for 48 h, following  
95 the similar protocol described above. After exposure, the cells were harvested and  
96 counted for the cell number (Countess II, Invitrogen, USA). An aliquot of the sample  
97 was submitted to cell lysis and protein concentration measurement using BCA kit  
98 (Thermo Fisher, USA). Another aliquot of cell sample ( $3 \times 10^6$  cells per group) was  
99 submitted to aqua regia digestion using previously-reported protocol,<sup>2</sup> and the as-  
100 prepared sample diluted with 3%  $\text{HNO}_3$  was quantitatively analyzed for Au contents  
101 using inductively coupled plasma-mass spectrometry (ICP-MS, Agilent 8800, USA).  
102 The final result of Au concentration was adjusted by protein concentration of each  
103 sample. The negative control of the mESCs without chemical treatment was set in  
104 parallel, and the negligible level of Au in this group confirmed no cross contamination  
105 during exposure experiments. The particle number of AuNPs per cell was estimated  
106 using Au concentration in each sample adjusted by cell number and the conversion  
107 coefficients of mass-to-particle for AuNPs, which were calculated by the following  
108 formula:

$$109 \quad \textit{Conversion coefficient} = \frac{\textit{Mass concentration (ng/mL)}}{\textit{Particle concentration (particles/mL)}}.$$

110 Wherein, the mass concentrations of AuNP-5, AuNP-20, and AuNP-80 were 1  
111  $\text{mg/mL}$ , and the particle concentrations were  $8.50 \times 10^{14}$ ,  $1.20 \times 10^{13}$ , and  $2.40 \times 10^{11}$   
112  $\text{particle/mL}$ , respectively, according to the vendor's manuals. The conversion  
113 coefficients of mass to particle were thus calculated to be  $1.18 \times 10^{-9}$ ,  $8.33 \times 10^{-8}$ ,  
114  $4.17 \times 10^{-6}$   $\text{ng/particle}$  for AuNP-5, AuNP-20 and AuNP-80, respectively.

115 **Alkaline phosphatase (AP) activity assay.** The mESCs seeded in 6-well plates were  
116 performed AuNP-exposure experiments (1  $\mu\text{g}/\text{mL}$  AuNPs, 48 h), following the  
117 similar protocol described above, or cultured for 48 h without any exposure (negative  
118 control). The cells were then fixed in citrate-acetone-formaldehyde buffer (citrate:  
119 acetone: formaldehyde = 5: 13: 2, v/v) for 30 seconds, followed by washing, alkaline  
120 dye staining and counterstaining with hematoxylin, according to the manual  
121 instruction of a commercially-available AP activity kit (Sigma, USA).<sup>3</sup> The pictures  
122 were imaged under an inverted microscope (Olympus IX73, Japan). The AP activity  
123 in each group was quantitatively evaluated by the grey values of stained cell clones  
124 with background subtraction using ImageJ (NIH, USA), and expressed as relative AP  
125 activity of the negative control.

126 **Transcriptional levels of pluripotency biomarkers.** After 1  $\mu\text{g}/\text{mL}$  AuNP  
127 treatments or naïve culture for 48 h, both the negative control and the exposed mESCs  
128 were harvested for RNA extraction with TRIZOL reagent (Invitrogen, USA)  
129 according to the vendor's instruction. After purification and quantitation, the mRNA  
130 sample (2  $\mu\text{g}$ ) was reversely-transcribed to cDNA using the one-step cDNA synthesis  
131 kit (Biorad, USA), and finally submitted to real time-polymerase chain reaction (RT-  
132 PCR) on a Roche 480 system (UK) with a SYBR green kit (Biorad, USA). The target  
133 genes included Nanog, Oct-4 and Sox-2, and GAPDH was used as the house-keeping  
134 gene. The sequences of forward and reverse primers in [Table S1](#) were designed  
135 according to previously-reported protocol.<sup>1</sup> The relative mRNA level was normalized  
136 by the Ct value of GAPDH using  $2^{-\Delta\Delta\text{Ct}}$  method.<sup>4</sup>

137 **Protein expressions of pluripotency biomarkers.** With the similar exposure  
138 protocol described above, the mESCs from different groups were lysed with ice-cold  
139 RIPA solution (Solarbio, China) containing  $1\times$  protease and phosphatase inhibitor  
140 (Cell signaling technology, USA). After centrifugation (15,000 g, 20 min), the protein  
141 concentration of each sample was determined by BCA kit (Thermo, USA). Suitable  
142 amount of protein samples from different treatments were submitted to Western blot  
143 assay. The primary antibodies included goat anti-Oct-4 (Abcam, ab27985), rabbit

144 anti-Nanog (Abcam, ab80892) and rabbit anti-GAPDH (Abcam, ab9485) and their  
145 dilution ratio was 1:1000. The corresponding horseradish peroxidase (HRP)-  
146 conjugated secondary antibodies were obtained from ZSGB-bio (China), and they  
147 were used at the ratios of 1:3000 to 1:5000. The target protein bands were developed  
148 onto X-ray films with ECL kit (Pierce, USA). The quantitative analysis was  
149 performed by measuring the grey densities of protein bands using ImageJ (NIH, USA),  
150 and the results were expressed as the relative values of the negative control.

151 **Isolation of small extracellular vesicles (sEVs).** The mESCs seeded in 6-well plates  
152 were processed for 48-h incubation in N2B27 medium with or without 1  $\mu\text{g}/\text{mL}$   
153 AuNPs (i.e. AuNP-5, AuNP-20 and AuNP-80). The protocol for sEV preparation  
154 from mESCs was referenced according to the previous study.<sup>5</sup> Briefly, after the  
155 removal of floating cells (400 g, 15 min), the culture medium was sequentially  
156 centrifuged under a series of conditions (i.e. 2000 g for 20 min, 10,000 g for 30 min)  
157 to remove the pellets of apoptotic body (AB) and microvesicle (MV) fractions,  
158 respectively. The supernatant was then concentrated using ultrafiltration (100 kDa,  
159 Merck Millipore, USA), filtrated using the 0.22- $\mu\text{m}$  sieve and finally centrifuged  
160 twice at 100,000 g for 90 min using an Optima L-100K ultracentrifuge equipped with  
161 70 Ti rotor (Beckman Coulter, USA). After transferring away the supernatant, the  
162 removal of AuNPs from sEVs was performed by centrifugation of the residue  
163 suspension under 12,500 g for 20 min, and the supernatant samples were sEVs,  
164 including sEV-ctrl, sEV-5, sEV-20 and sEV-80, respectively, which contained  
165 undetectable Au levels measured by ICP-MS. The above processes were carried out at  
166 4  $^{\circ}\text{C}$ , and the average protein concentrations of the prepared sEV suspensions were  
167 about 600  $\mu\text{g}/\text{mL}$  after sample lysis and protein quantification using BCA kit (Thermo,  
168 USA).

169 **Characterization of sEVs.** The sEV samples fixed in 2% PFA were transferred onto  
170 carbon membrane-coated copper grids, and air-dried for 20 min. The samples were  
171 washed with PBS, and further fixed with 1% glutaraldehyde for 5 min followed by  
172 negatively staining with 1% uranylacetate for 1 min.<sup>5</sup> Images were obtained on a

173 TEM (JEOL H7500, Japan) at an accelerating voltage of 80 kV.

174 **Analysis of sEV protein biomarkers.** The isolated sEVs were lysed for protein  
175 quantification, and submitted to Western blot following the similar protocol  
176 mentioned above. The primary antibodies included rabbit anti-CD63 (Abcam, 1:1000),  
177 rabbit anti-HSP70 (Cell signaling, 1:1000), rabbit anti-Flotillin-1 (Cell signaling,  
178 1:1000), and rabbit anti-Calreticulin (Cell signaling, 1:1000). As the protein  
179 biomarker of calreticulin was not expressed in sEVs, it was tested herein to confirm  
180 no contamination from other cell components in sEV samples.

181 **Immunostaining analysis of sEVs.** Total 5  $\mu$ L of sEV suspensions (600  $\mu$ g  
182 protein/mL) were incubated with PE-CD63 antibody (1:100, Biolegend, CA) at 37 °C  
183 for 40 min in darkness.<sup>6, 7</sup> Then the sEVs were centrifuged at 100,000 g for 90 min.  
184 The pellets of sEVs were re-suspended in PBS, and dropped onto the gelatin pre-  
185 coated slides, and finally sealed with cover slips by nail polish. The as-prepared  
186 samples were imaged by a Leica TCS-SP5 confocal microscopy (Germany).

187 **Particle size and concentration analysis of sEVs.** The particle size and particle  
188 concentration measurements of sEVs were conducted on a nanoparticle tracking  
189 analysis system (NTA, NS300, Malvern, UK) configured with 640 nm laser. Briefly,  
190 10  $\mu$ L of sEVs (i.e. sEV-ctrl, sEV-5, sEV-20 and sEV-80) were either treated with 0.1%  
191 (v/v) Triton-X100 for 10 min at room temperature for background measurement of  
192 non-membrane particles,<sup>8</sup> or diluted with PBS to 1 mL,<sup>9</sup> then introduced manually  
193 with a syringe. Videos of 30-s duration of each sEV sample was recorded  
194 independently for 3 times, and the camera parameters, including camera level of 4,  
195 camera gain of 16, and threshold of 4, were set for all experiments. The mobility  
196 trajectories of sEVs with different sizes (including 30 nm, 60 nm, 90 nm, 120 nm and  
197 150 nm) were recorded, and the related data analysis was performed using NTA  
198 software (version 2.3, Malvern, UK) to obtain the concentrations of particles ( $C_p$ ) and  
199 non-membrane particles ( $C_{NMP}$ ). To evaluate the correlation between protein levels of  
200 sEVs and their particle concentrations, two aliquots of the samples from different  
201 groups were submitted to gradient dilution, and performed RIPA lysis for protein

202 quantitation using BCA kit (Thermo, USA) and NTA measurement, respectively. The  
203 linear correlations were simulated for different sEV samples by Origin85 software,  
204 and compared with each other. The purities of sEVs from different groups were  
205 calculated by the following equation:

$$206 \quad \text{Purity} = (1 - C_{\text{NMP}}/C_{\text{P}}) \times 100\%$$

207 **Quartz crystal microbalance with dissipation (QCM-D) monitoring.** sEV rigidity  
208 and deposition mass were recorded by a Q-sense E4 system (Biolin Scientific AB,  
209 Sweden). The QCM-D measurements were performed as follows. First, a cleaned  
210 SiO<sub>2</sub> sensor was pre-coated by poly-lysine solution (PLL, 0.1% w/v, Solabio, China)  
211 until both  $\Delta$ Frequency ( $\Delta F$ ) and  $\Delta$ Dissipation ( $\Delta D$ ) approached to stable baselines.  
212 Next, Tris-HCl buffer (10 mM Tris-HCl, 150 mM NaCl, pH 7.4)<sup>10</sup> was introduced to  
213 remove unbound PLL for another steady baseline. Then, sEVs suspended in Tris-HCl  
214 buffer (1:50) were injected into chamber with the continuous record at the third to the  
215 eleventh overtones. In all steps, the flow rate was set at 50  $\mu$ L/min,<sup>11</sup> and the  
216 temperature was maintained at 37 °C. The data were collected and condensed at the  
217 fifth overtone by QTools software (Version 3.0.17).

218 **Label-free proteomics analysis.** Three batches of sEV-ctrl and sEV-5 samples were  
219 lysed in SDT buffer (100 mM Tris-HCl containing 4% w/w sodium dodecyl sulfate  
220 and 0.1 M dithiothreitol, pH 7.6), and sonicated on ice for 20 s. The samples were  
221 then heated at 60 °C under shaking for 30 min followed by a series of sonication to  
222 obtain homogenate. After the protein quantitation, 90  $\mu$ g protein from each sample  
223 was extracted with filter (10 kDa, Millipore). According to previously-reported  
224 protocol,<sup>12</sup> the protein lysates were mixed with 200  $\mu$ L of 8 M urea in ultrafilter tubes,  
225 followed by ultracentrifugation-based concentration (14000 g, 40 min) and SDT  
226 buffer washing. Then the concentrate was digested overnight with trypsin (1:25, w/w),  
227 and the generated peptides were lyophilized, resolved in Milli-Q water and desalted  
228 with MILI-SPE C<sub>18</sub> column (Millipore). The peptides were elicited by 80%  
229 acetonitrile. After being lyophilized, the peptide samples were re-suspended in 0.1%  
230 formic acid, and submitted to the analysis using high performance liquid



231 chromatography (HPLC, EASY nLC-1000) coupled with a Q Exactive Orbitrap Mass  
232 spectrometer (Thermo Scientific, USA). The HPLC system included a Pepmap 100  
233 column (Thermo Scientific, 100  $\mu\text{m} \times 2 \text{ cm}$ ) connected with an EASY column  
234 (Thermo Scientific, 10 cm, ID 75  $\mu\text{m}$ , C<sub>18</sub>-A2). The mobile phase was consisted of  
235 de-ionized water containing 0.1% formic acid (phase A, 16%) and acetonitrile  
236 containing 0.1% formic acid (phase B, 84%), and the flow rate was 300 nL/min.<sup>8</sup>  
237 Mass spectra with the scanning range of  $m/z$  300-1800 at the resolution of 70,000  
238 were obtained under positive ion mode. Data-dependent scan mode was used by  
239 selecting the top 20 abundant ions for fragmentation under the normalized collision  
240 energy of 30 eV.

241 All peptides data were analyzed using the MaxQuant software (v. 1.5.3.17).  
242 Carbamidomethylation of cysteines and methionine oxidation were set as fixed  
243 modification and variable modification, respectively. Trypsin was selected as the  
244 enzyme, with max missed cleavages of two. Peptide and fragment ion tolerances were  
245 6 part per million (ppm) and 20 ppm, respectively. The database incorporated both the  
246 forward and reversed sequences to allow the determination of false discovery rate  
247 (FDR) of 1% at peptide-spectrum match, peptide, and protein levels. Only proteins in  
248 sEV-5 with the abundance higher than 1.5-fold or less than 0.67-fold of that of sEV-  
249 ctrl and  $p$  value less than 0.05 were considered to be differentially-expressed. Protein  
250 clustering analysis was performed on R package of complex heatmap. The clustering  
251 distance and method were set to Euclidean and average linkage, respectively.  
252 Bioinformatics analysis of the results was conducted using the Blast2GO algorithm to  
253 obtain the overall GO analysis, including procedures of blast, mapping, annotation  
254 and annotation augmentation.

255 **4T1 cell culture and proliferation experiment.** 4T1 cells were purchased from  
256 Institute of Basic Medical Sciences, Chinese Academy of Medical Sciences. The cells  
257 were cultured in DMEM medium supplemented with 10% fetal bovine serum (FBS,  
258 Gibco, USA) and 1% penicillin and streptomycin (Gibco, USA) at 37 °C and 5% CO<sub>2</sub>.  
259 When sEV exposure experiments were performed, DMEM medium containing 10%

260 EV-free fetal bovine serum (D-FBS, Vivacell, USA) and 1% penicillin and  
261 streptomycin (Gibco, USA) was used for cell incubation. Both FBS and D-FBS (10%  
262 in DMEM medium) were submitted to particulate measurement using a Nano ZS  
263 system (Malvern, UK) under the similar condition described above, showing the  
264 negligible shielding influences from particles in D-FBS (Fig. S11A). The cell  
265 viabilities of 4T1 using alamarBlue assay remained the same after 24-h culture in both  
266 kinds of culture medium (Fig. S11B), confirming cell viability was not influenced by  
267 D-FBS-supplemented culture medium.

268 As for the effects of sEVs on 4T1 cell proliferation, the cells were seeded on 96-well  
269 plate at the density of  $1 \times 10^4$  cells per well and cultured in 10% FBS-supplemented  
270 DMEM medium (i.e. complete medium) for 24 h. Then the medium was replaced by  
271 10% D-FBS-supplemented DMEM medium (i.e. EV free medium) containing  
272 different concentrations of sEVs (30  $\mu\text{g}/\text{mL}$ , 50  $\mu\text{g}/\text{mL}$ , and 100  $\mu\text{g}/\text{mL}$ ) derived from  
273 different groups of mESCs (e.g. sEV-ctrl, sEV-5, sEV-20 and sEV-80). The exposure  
274 lasted for 24 h, and the final cell proliferation was analyzed, according to the protocol  
275 used in mESC viability experiments.

276 **Flow cytometry analysis for cell apoptosis.** The cell apoptosis was measured by a  
277 dead cell apoptosis kit with Annexin V-FITC and PI (Invitrogen, USA). In brief, 4T1  
278 cells cultured in 24-well plates at the density of  $2 \times 10^5$  cells per well were exposed to  
279 sEV-ctrl and sEV-5 for 24 h. The negative control without any treatment was set in  
280 parallel. After exposure, the cells were harvested and washed with cold PBS. Then,  
281 the cell suspensions were incubated with Annexin V-FITC and PI solutions (100  
282  $\mu\text{g}/\text{mL}$ ) for 15 min. The stained cells were finally analyzed on a flow cytometry  
283 (Novocyte, ACEA, USA) at the wavelengths ( $\lambda_{\text{excitation}}/\lambda_{\text{emission}}$ ) of 488 nm/519  
284 nm and 561 nm/615 nm, respectively.

285 **Cellular uptake of sEVs in 4T1 cells based on morphological observation.** The  
286 samples of sEV-ctrl and sEV-5 (30  $\mu\text{g}/\text{mL}$ ) were labeled with 1  $\mu\text{M}$  1,1'-dioctadecyl-  
287 3,3,3',3'-tetramethylindodicarbonyanepchlorate (DiD, Thermo Fish, USA), a kind  
288 of lipophilic carbocyanine fluorescent dyes by 1-h incubation at 37 °C, according to

289 the previously-reported protocol.<sup>13</sup> The mixture was diluted (1:1000) with fresh D-  
290 FBS medium and processed ultrafiltration centrifugation (10 kDa, Millipore, 14000 g,  
291 30 min) to remove excess probes for the following cell exposure tests.

292 4T1 cells were seeded onto the glass chamber slides (Lab-Tek, Thermo Fisher, USA)  
293 at the density of  $2 \times 10^4$  cells per well. After 24-h incubation in D-FBS medium, the  
294 cells were labeled by 5  $\mu\text{M}$  3,3'-dioctadecyloxacarbocyanine perchlorate (DiO,  
295 Thermo Fisher, USA) at 37 °C for 15 min, then washed by D-FBS medium for 3 times.  
296 The DiD-labeled sEVs were added to the cell cultures and incubated for 6 h. The cells  
297 were finally fixed in 4 % PFA for 20 min, and mounted with VECTASHIELD anti-  
298 fade mounting medium containing DAPI (H-1200, Vector Laboratories, CA).<sup>14</sup> The  
299 fluorescent images were obtained using a Leica SP5 confocal microscopy (Germany)  
300 with excitation lasers of 405 nm (DAPI), 488 nm (DiO), and 633 nm (DiD), and the  
301 corresponding emission signals were collected at 420-470 nm, 500-600 nm and 700-  
302 800 nm, respectively.

303 **Flow cytometry analysis of sEV uptake by 4T1 cells.** 4T1 cells were cultured in 12-  
304 well plates at the density of  $1 \times 10^5$  cells per well for 24 h and DiD-labeled sEV-ctrl  
305 and sEV-5 samples (30  $\mu\text{g}/\text{mL}$ ) were added and incubated for 6 h. The negative cell  
306 control without sEVs was designed in parallel. After wash with cold PBS, the cells  
307 were re-suspended at a density of  $2 \times 10^5$  cells/mL and submitted to flow cytometry  
308 analysis (BD, LSR II, USA). Forward scatter (FSC) and side scatter (SSC) signals  
309 were collected using 488 nm laser, while DiD fluorescence channel (695/40) were  
310 assessed with 633 nm laser. All threshold gates were set based on control cells, and  
311 temperature was maintained at 4°C.

312 **Wound healing assays.** 4T1 cells were seeded into 6-well plates with a culture-insert  
313 in each well (ibidi GmbH, Germany). The cell density was  $5.6 \times 10^5$  cells/insert, and  
314 the culture was performed in the complete medium for 24 h. The insert was then  
315 removed quickly, leaving a cell-free gap with the width of 500  $\mu\text{m}$ , and each well was  
316 gently washed by PBS twice to remove the floating cells. The cells were exposed to  
317 FBS-free medium containing 30  $\mu\text{g}/\text{mL}$  sEVs (i.e. sEV-ctrl, sEV-5, sEV-20 and sEV-

318 80) for 12 h, respectively. The negative cell control without sEVs was set in parallel.  
319 The migration of cells in the gap area was pictured by Olympus microscopy (IX73,  
320 Japan). The migration index (M) was calculated as follows:

$$M = 1 - \frac{A_{12}}{A_0}$$

321

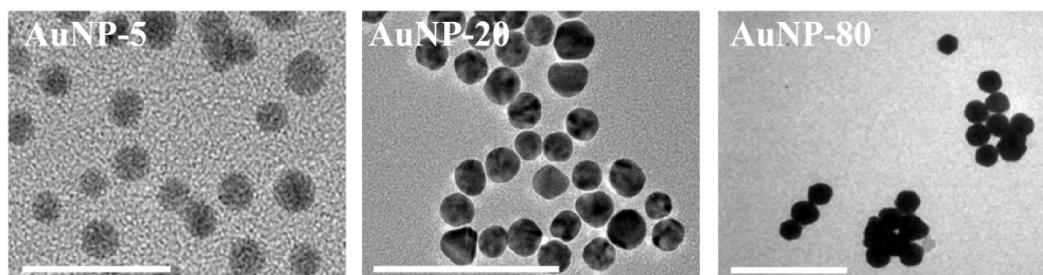
322 Where  $A_0$  is the initial wound area and  $A_{12}$  represents the remaining wound area after  
323 12-h treatment. All data calculation was acquired using ImageJ (NIH, USA). The M  
324 values were calculated and statistically compared for different sEV treatments.

325 **Assay for protein biomarkers regulating 4T1 cell migration.** 4T1 cells were  
326 seeded in 24-well plates at a density of  $2 \times 10^5$  cells per well, and cultured for 24 h.  
327 The exposure was subsequently performed by stimulating the cells with 50  $\mu\text{g}/\text{mL}$   
328 sEVs (i.e. sEV-ctrl, sEV-5) for 6 h. The negative control without any treatment was  
329 set in parallel. After wash with ice-cold PBS, the cells were lysed in RIPA solution  
330 and quantitatively measured for protein concentration. The as-prepared samples were  
331 submitted to Western blot assay following the protocol described above. The primary  
332 antibodies included rabbit anti-Erk 1/2 (Cell signaling, 1:1000), rabbit anti-  
333 phosphoErk 1/2 (Cell signaling, 1:1000), rabbit anti-cofilin (Cell signaling, 1:1000),  
334 and rabbit anti-GAPDH (Cell signaling, 1:1000).

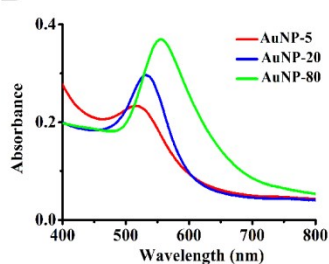
335 **Statistical analysis.** All experiments were independently carried out at least for three  
336 times, and the final results were represented as mean values  $\pm$  standard deviations  
337 (SDs). The graphs were plotted using GraphPad Prism 7. One-way analysis of  
338 variance (ANOVA) with the Bonferroni multi-group comparison test was used for the  
339 difference analysis of different groups, and the  $p$  value less than 0.05 (\*) or 0.01 (\*\*)  
340 was considered to be significantly different.

342 **Supplementary Figures**

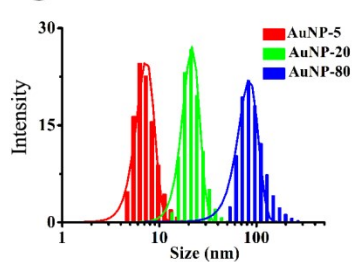
**A**



**B**



**C**



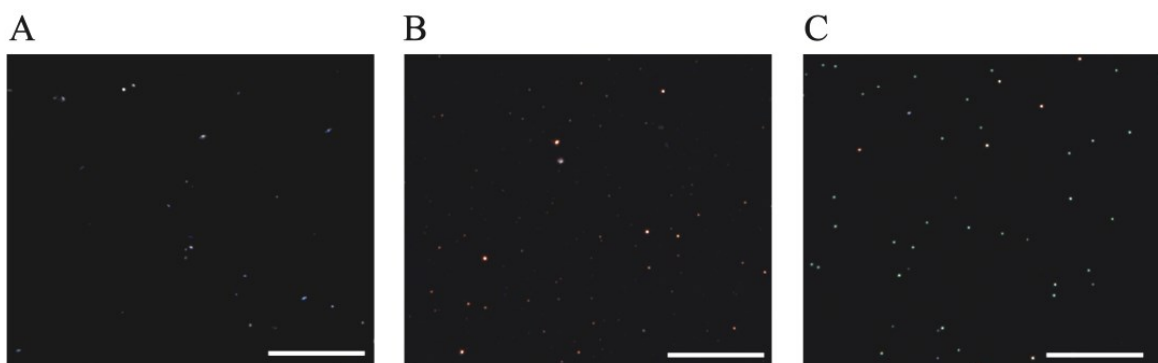
**D**

	Zeta potential (mV)
AuNP-5	$-22.01 \pm 1.81$
AuNP-20	$-32.17 \pm 2.19$
AuNP-80	$-55.21 \pm 7.34$

343

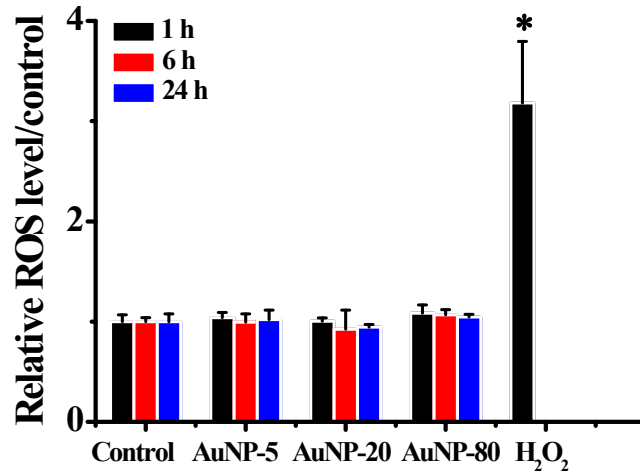
344 **Fig. S1 Characterization of the test AuNPs ( $n = 3$ ).** (A) TEM graphs of AuNP-5,  
 345 AuNP-20, and AuNP-80. Scale bars represent 20 nm for AuNP-5, 100 nm for AuNP-  
 346 20 and 500 nm for AuNP-80, respectively. (B) Localized surface plasmon resonance  
 347 absorption spectra of the test AuNPs. (C) Hydrodynamic sizes of the AuNPs. (D) Zeta  
 348 potentials of the AuNPs.

349



350

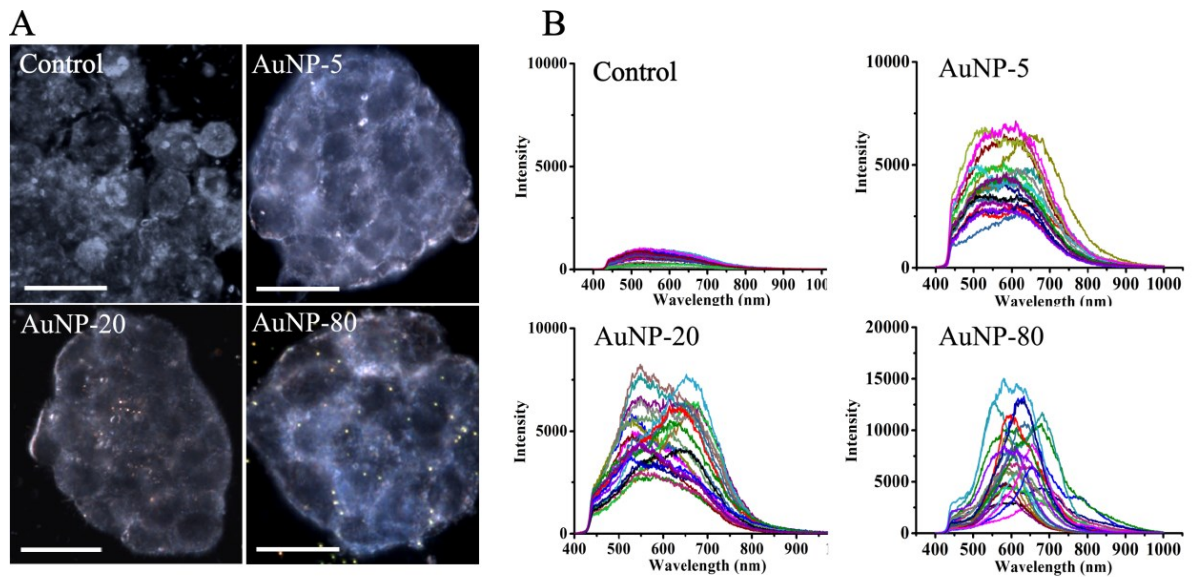
351 **Fig. S2 Enhanced dark-field images for the test AuNPs.** (A) AuNP-5. (B) AuNP-  
 352 20. (C) AuNP-80. Scale bars represent 25  $\mu\text{m}$ .



353

354 **Fig. S3 ROS generation in mESCs from different groups ( $n = 3$ ).  $*p < 0.05$  versus**  
 355 the control.

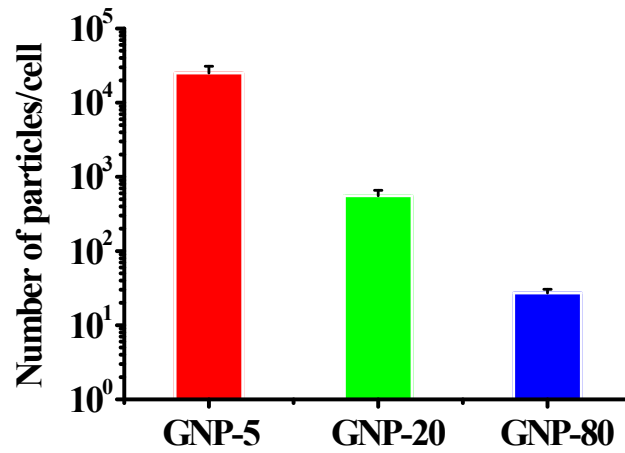
356



357

358 **Fig. S4 Cellular uptake of AuNPs by the mESCs.** (A) Dark-field images for control  
 359 and AuNP-treated cells. The scale bars show 25  $\mu\text{m}$ . (B) The normalized  
 360 hyperspectral scattering signals of AuNPs in the mESCs. The intensities of AuNP  
 361 exposure groups were higher than 2500, whereas that of the negative control was  
 362 below 700, which was similar to the previously-reported finding.<sup>15</sup> Meanwhile, the  
 363 scattering peaks of the adsorption spectrums were widened in AuNP-exposure groups,  
 364 showing the potential aggregation of AuNPs in cells.<sup>16</sup>

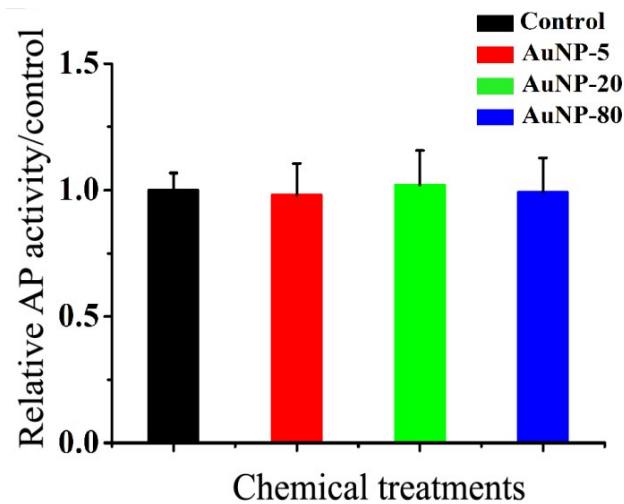
365



366

367 **Fig. S5** The calculated AuNP numbers per cell in different exposure groups.

368



369

370 **Fig. S6** Relative AP activities of mESCs with AuNP treatments ( $n = 3$ )

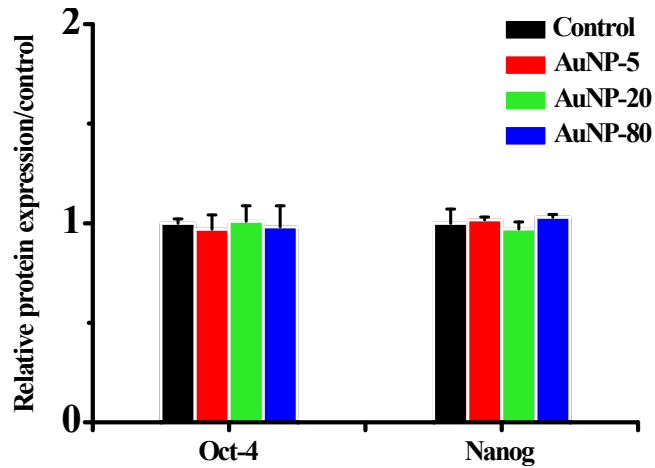
371

372 **Table S1.** The primer sequences for RT-PCR analysis.

Gene name	Sequence of the primers (5'-3')	
	Forward	Reverse
GAPDH	CCTGCGACTTCAACAGCAAC	TAGGGCCTCTCTTGCTCAGT
Oct4	TGGATCCTCGAACCTGGCTA	CTCAGGCTGCAAAGTCTCCA
Nanog	GGAGGACTTTCTGCAGCCTT	TGCCCTGACTTTAAGCCCAG
Sox2	AACCGATGCACCGCTACGA	TGCTGCGAGTAGGACATGCTG

373

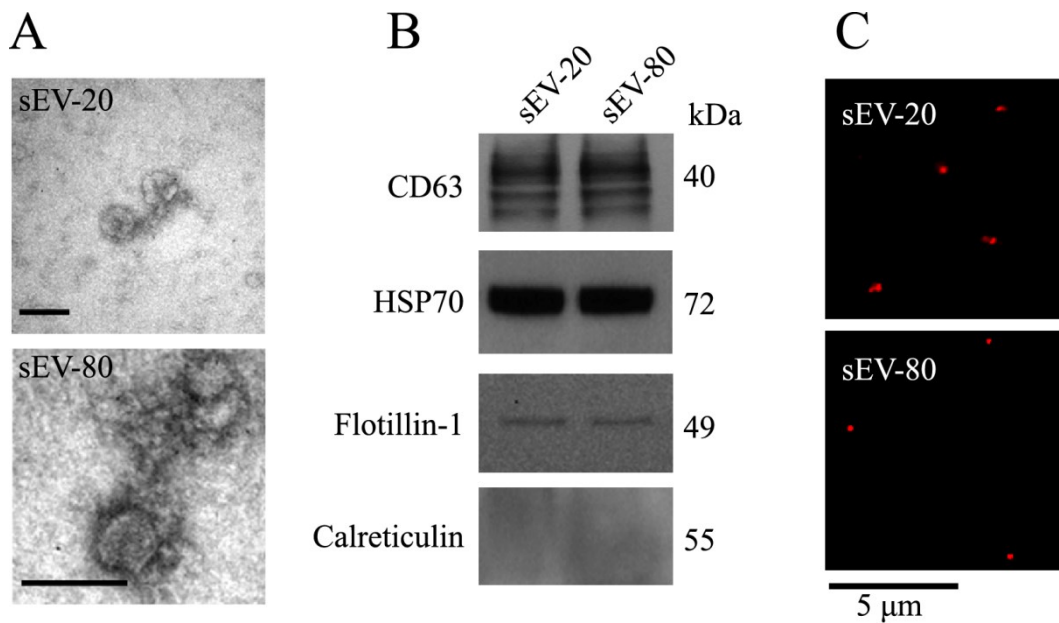
374



375

376 **Fig. S7** Relative protein expressions of pluripotency biomarkers in the mESCs (*n*  
377 = 3).

378

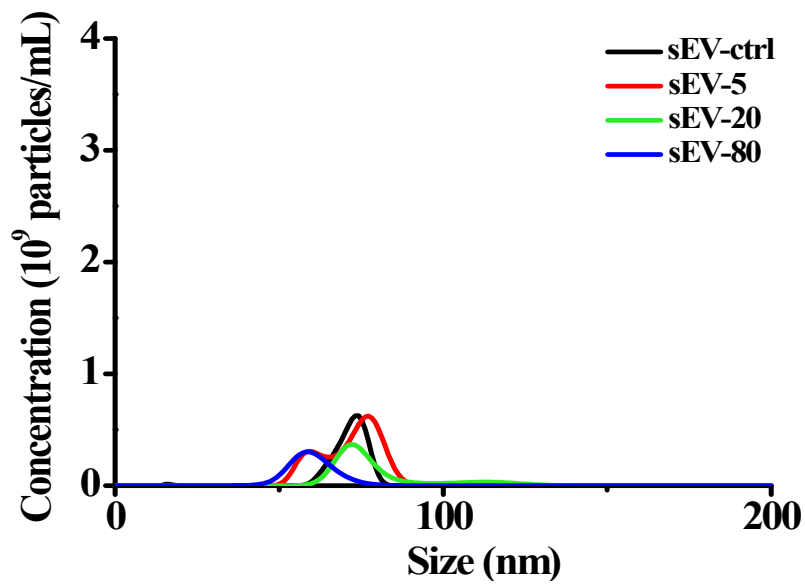


379

380 **Fig. S8** Characterization of sEV-20 and sEV-80. (A) TEM images (Scale bars =  
381 100 nm). (B) Western blots for the protein markers. (C) Immunoblotting of CD63 in  
382 sEVs (Scale bar = 5 μm).

383

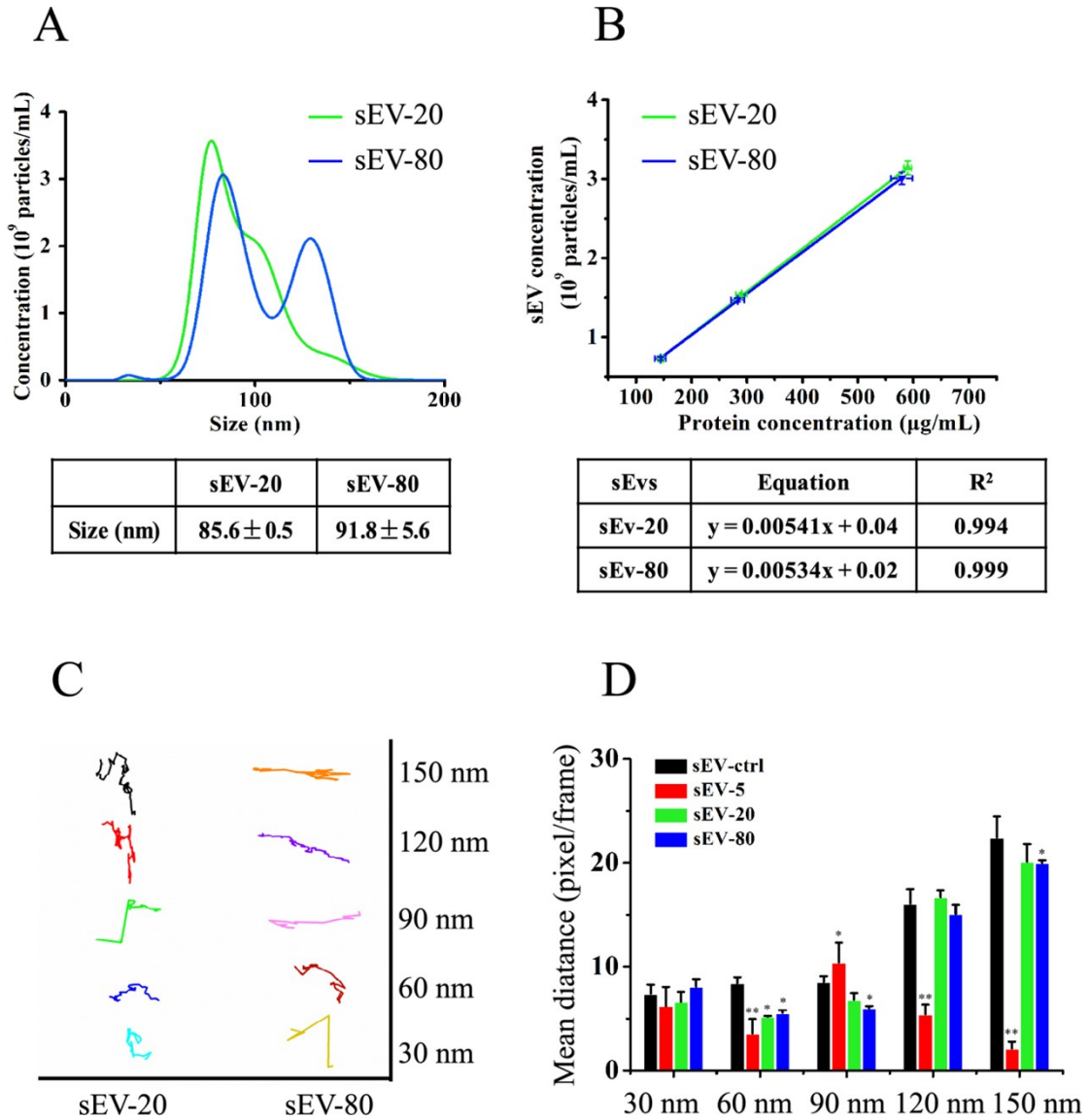




384

385 **Fig. S9 NTA data for non-membrane particles in sEV samples.** The pretreatment  
386 of 0.1% Triton-X100 was performed for sEVs to obtain non-membrane particles.<sup>8</sup>

387



388  
389

390 **Fig. S10 Characterization of sEV-20 and sEV-80** ( $n = 3$ ). (A) The hydrodynamic  
391 sizes. (B) Linear correlation between particle concentrations and protein contents of  
392 sEVs. (C) Typical mobility trajectories of sEVs with different sizes from NTA assay.  
393 (D) The mean trajectory distances of sEVs with different sizes. \* $p < 0.05$ , and \*\* $p <$   
394  $0.01$  versus sEV-ctrl.

395

396 **Table S2. The purities of sEVs from different groups.**

	sEV-ctrl	sEV-5	sEV-20	sEV-80
$C_p$ (particles/mL)	$5.5 \times 10^{10}$	$7.3 \times 10^{10}$	$8.3 \times 10^{10}$	$6.6 \times 10^{10}$
$C_{NMP}$ (particles/mL)	$1.6 \times 10^9$	$3.2 \times 10^9$	$3.8 \times 10^9$	$1.8 \times 10^9$
Purity	97%	96%	95%	97%

397

398

399 **Table S3. The specifically-expressed proteins in sEV-ctrl or sEV-5.**

Protein	Protein Name	Gene Name	Coverage/%
B9EJV3	GREB1-like protein	Greb11	1.6
O09118	Netrin-1	Ntn1	9.6
O09167	60S ribosomal protein L21	Rpl21	11.2
P10711	Transcription elongation factor A protein 1	Tcea1	4
P27048	Small nuclear ribonucleoprotein-associated protein B	Snrpb	10
P62196	26S proteasome regulatory subunit 8	Psmc5	7.4
P62889	60S ribosomal protein L30	Rpl30	13.9
P63325	40S ribosomal protein S10	Rps10	5.5
P97379	Ras GTPase-activating protein-binding protein 2	G3bp2	6
Q08943	FACT complex subunit SSRP1	Ssrp1	2.4
Q8BHW2	Protein OSCP1	Oscp1	7.1
A2ASQ1	Agrin	Agrn	1.6
P23242	Gap junction alpha-1 protein	Gja1	15.2
Q3TYQ9	Aldehyde oxidase 4	Aox4	1.9
Q8QZY6	Tetraspanin-14	Tspan14	10.4
Q9ESU6	Bromodomain-containing protein 4	Brd4	1

400

401

402 **Table S4. The differentially-expressed proteins in sEV-5 compared with sEV-ctrl.**

Protein	Protein Name	Gene Name	Coverage/%	$FC_{sEV-5/sEV-ctrl}^a$	t test p value
P14115	60S ribosomal protein L27a	Rpl27a	22.3	3.1204	0.0161
P49312	Heterogeneous nuclear ribonucleoprotein A1	Hnrnpa1	13.1	2.8109	0.0055
P27659	60S ribosomal protein L3	Rpl3	7.9	2.0963	0.0137
P10126	Elongation factor 1-alpha 1	Eef1a1	39.6	2.0143	0.0438
Q61937	Nucleophosmin	Npm1	22.9	1.9476	0.0500
P47911	60S ribosomal protein L6	Rpl6	12.2	1.8238	0.0270
Q02248	Catenin beta-1	Ctnnb1	4.5	0.6508	0.0005
Q8VDN2	Sodium/potassium-transporting ATPase subunit alpha-1	Atp1a1	17	0.5981	0.0380
Q9WU78	Programmed cell death 6-interacting protein	Pdcd6ip	31.9	0.5961	0.0470
O35874	Neutral amino acid transporter A	Slc1a4	4.9	0.5558	0.0500
Q80UG2	Plexin-A4	Plxna4	1.1	0.4514	0.0457
P09242	Alkaline phosphatase, tissue-nonspecific isozyme	Alpl	27.1	0.2779	0.0133
P14094	Sodium/potassium-transporting ATPase subunit beta-1	Atp1b1	17.8	0.2349	0.0467

403

404 <sup>a</sup>  $FC_{sEV-5/sEV-ctrl}$  is the fold change of the protein abundance in sEV-5 versus that of

405 sEV-ctrl.

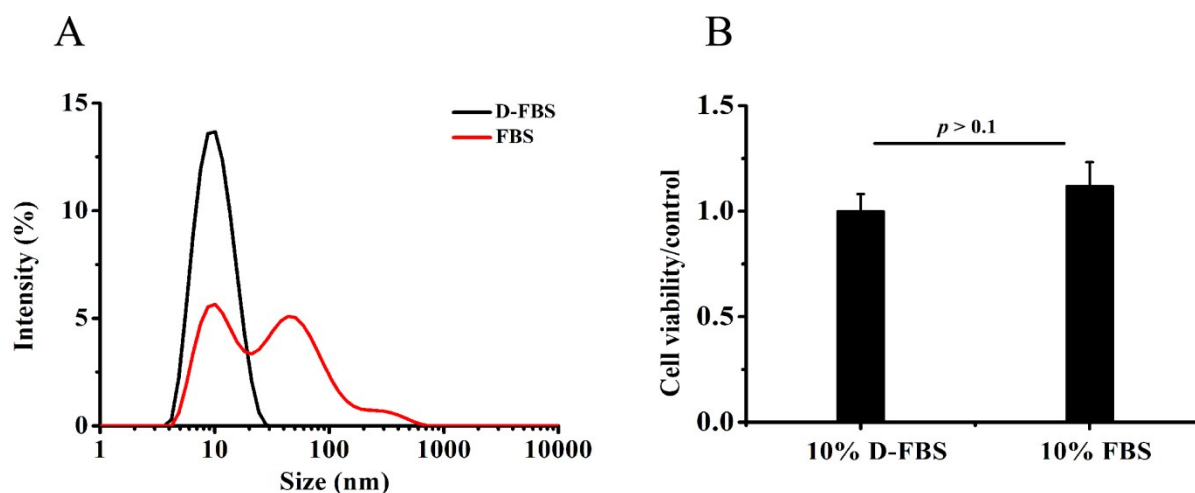
406

407 **Table S5. GO enrichment analysis.**

GO ID	Signaling pathway	Category	Protein
GO:0014704	Intercalated disc	Cell component	P23242,Q02248,P14094,Q8VDN2
GO:0044291	Cell-cell contact zone	Cell component	P14094,P23242,Q02248,Q8VDN2
GO:0061695	Transferase complex	Cell component	P62196,Q9ESU6,P10711
GO:0008023	Transcription elongation factor complex	Cell component	Q9ESU6,Q08943
GO:0016591	RNA polymerase II	Cell component	P10711,P62196
GO:0005667	Transcription factor complex	Cell component	Q02248,Q62318,P10711,P62196
GO:0000049	tRNA binding	Molecular function	P10126,P47911,P63325
GO:0060590	ATPase regulator activity	Molecular function	P14094,A2ASQ1
GO:0019829	Cation-transporting ATPase activity	Molecular function	P14094,Q8VDN2
GO:0022853	Active ion transmembrane transporter activity	Molecular function	P14094,Q8VDN2
GO:0015662	ATPase activity, coupled to transmembrane movement	Molecular function	P14094,Q8VDN2
GO:0042625	ATPase coupled ion transmembrane transporter activity	Molecular function	P14094,Q8VDN2
GO:0008016	Regulation of heart contraction	Biological process	Q8VDN2,P14094,A2ASQ1,P23242
GO:0036376	Sodium ion export	Biological process	A2ASQ1,P14094,Q8VDN2
GO:0140115	Export across plasma membrane	Biological process	P14094,Q8VDN2,A2ASQ1
GO:0060047	Heart contraction	Biological process	Q8VDN2,P23242,P14094,A2ASQ1
GO:0035725	Sodium ion transmembrane transport	Biological process	P14094,Q8VDN2,A2ASQ1
GO:0086009	Membrane repolarization	Biological process	P23242,P14094,Q8VDN2
GO:0071804	Cellular potassium ion transport	Biological process	P14094,A2ASQ1,Q8VDN2
GO:0071260	Cellular response to mechanical stimulus	Biological process	P23242,Q02248,Q8VDN2

408

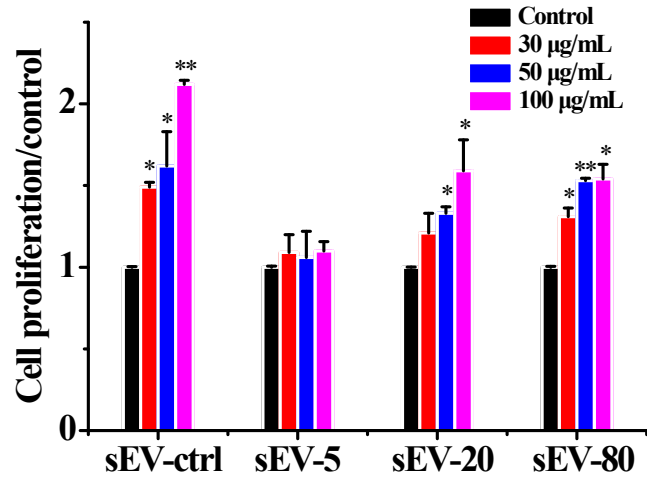
409



410

411 **Fig. S11 Comparison of D-FBS with normal FBS.** (A) Hydrodynamic sizes of  
 412 particulate matters in FBS and D-FBS at 25 °C. Several peaks appeared in the range of  
 413 1 nm - 400 nm in normal FBS sample, showing the existence of various EVs,<sup>17</sup>  
 414 whereas, only a single peak with the intensity less than 15% was detected in D-FBS,  
 415 indicating most of the EVs were removed. (B) Cell viabilities of 4T1 in DMEM  
 416 medium supplemented with 10% FBS or 10% D-FBS ( $n = 3$ ). No significant  
 417 difference was observed between these two groups ( $p > 0.1$ ).

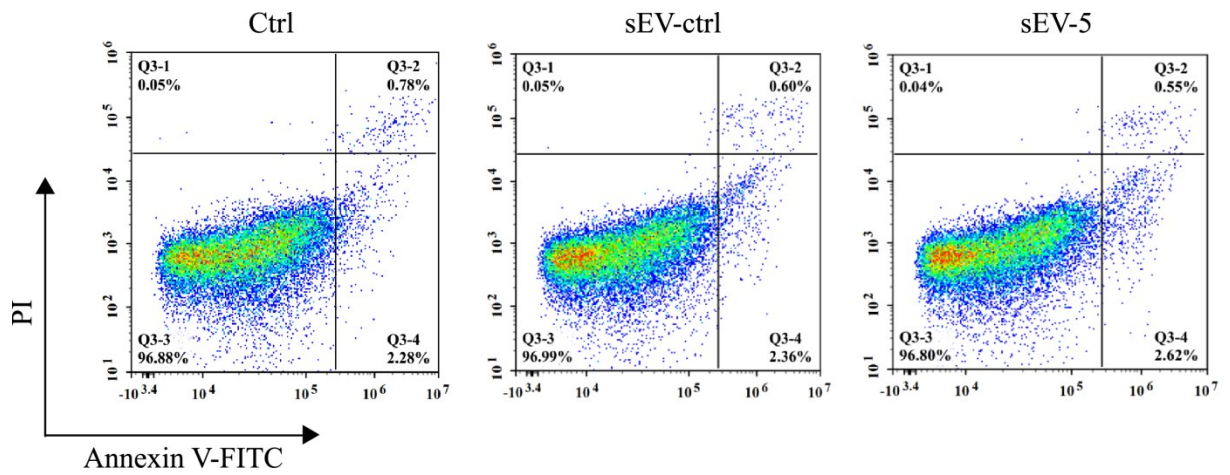
418



419

420 **Fig. S12** The relative cell proliferation of 4T1 treated with sEVs ( $n = 3$ ). \*  $p <$   
 421 0.05, and \*\*  $p < 0.01$  versus control.

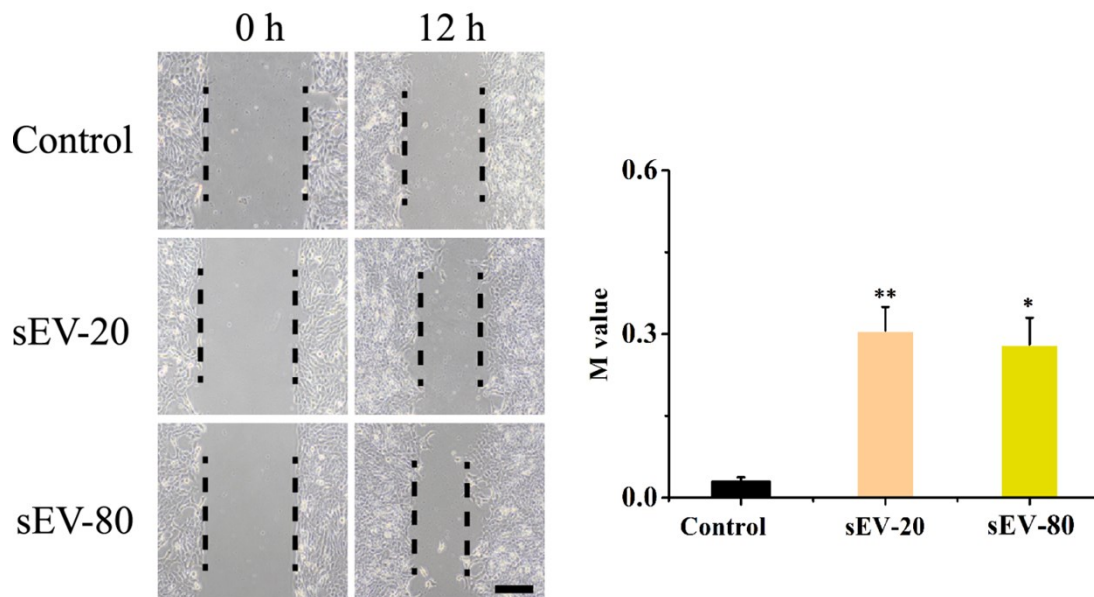
422



423

424 **Fig. S13** Cell apoptosis analysis of 4T1 cells in different groups.

425



426

427 **Fig. S14 Wound healing assays for 4T1 cells treated with sEV-20 and sEV-80** ( $n =$   
 428 3). The images were obtained at 0 h and 12 h, and the scale bar represents 200  $\mu\text{m}$ .  $*p$   
 429  $< 0.05$ ,  $**p < 0.01$  versus control.

430

#### 431 References

- 432 1 X. Yang, T. Ku, Z. Sun, Q. S. Liu, N. Yin, Q. Zhou, F. Faiola, C. Liao and G.  
 433 Jiang, *Toxicol. Lett.*, 2019, **312**, 139-147.
- 434 2 F. Hao, X. Jin, Q. S. Liu, Q. Zhou and G. Jiang, *ACS Appl. Mater. Interfaces*,  
 435 2017, **9**, 42577-42588.
- 436 3 N. Yin, S. Liang, S. Liang, R. Yang, B. Hu, Z. Qin, A. Liu and F. Faiola,  
 437 *Environ. Sci. Technol.*, 2018, **52**, 5459-5468.
- 438 4 X. Yang, W. Song, N. Liu, Z. Sun, R. Liu, Q. S. Liu, Q. Zhou and G. Jiang,  
 439 *Environ. Sci. Technol.*, 2018, **52**, 850-858.
- 440 5 C. Théry, S. Amigorena, G. Raposo and A. Clayton, *Curr. Protoc. Cell Biol.*,  
 441 2006, **30**, 3.22. 21-23.22. 29.
- 442 6 V. Pospichalova, J. Svoboda, Z. Dave, A. Kotrbova, K. Kaiser, D. Klemova, L.  
 443 Ilkovics, A. Hampl, I. Crha, E. Jandakova, L. Minar, V. Weinberger and V.  
 444 Bryja, *J. Extracell. Vesicles*, 2015, **4**, 25530.
- 445 7 Y. Tian, L. Ma, M. Gong, G. Su, S. Zhu, W. Zhang, S. Wang, Z. Li, C. Chen, L.

- 446 Li, L. Wu and X. Yan, *ACS Nano*, 2018, **12**, 671-680.
- 447 8 D. K. Jeppesen, A. M. Fenix, J. L. Franklin, J. N. Higginbotham, Q. Zhang, L. J.  
448 Zimmerman, D. C. Liebler, J. Ping, Q. Liu, R. Evans, W. H. Fissell, J. G. Patton,  
449 L. H. Rome, D. T. Burnette and R. J. Coffey, *Cell*, 2019, **177**, 428-445.e418.
- 450 9 I. Keklikoglou, C. Cianciaruso, E. Güç, M. L. Squadrito, L. M. Spring, S.  
451 Tazzyman, L. Lambein, A. Poissonnier, G. B. Ferraro, C. Baer, A. Cassará, A.  
452 Guichard, M. L. Iruela-Arispe, C. E. Lewis, L. M. Coussens, A. Bardia, R. K.  
453 Jain, J. W. Pollard and M. De Palma, *Nat. Cell Biol.*, 2019, **21**, 190-202.
- 454 10 N.-J. Cho, C. W. Frank, B. Kasemo and F. Höök, *Nat. Protoc.*, 2010, **5**, 1096-  
455 1106.
- 456 11 J. A. Jackman, S. Yorulmaz Avsar, A. R. Ferhan, D. Li, J. H. Park, V. P.  
457 Zhdanov and N.-J. Cho, *Anal. Chem.*, 2017, **89**, 1102-1109.
- 458 12 J. R. Wiśniewski, A. Zougman, N. Nagaraj and M. Mann, *Nat. Methods*, 2009, **6**,  
459 359.
- 460 13 C. Liu, J. Zhao, F. Tian, J. Chang, W. Zhang and J. Sun, *J. Am. Chem. Soc.*, 2019,  
461 **141**, 3817-3821.
- 462 14 Y. Ofir-Birin, P. Abou karam, A. Rudik, T. Giladi, Z. Porat and N. Regev-  
463 Rudzki, *Front. Immunol.*, 2018, **9**, 1011.
- 464 15 E. S. Oh, C. Heo, J. S. Kim, M. Suh, Y. H. Lee and J.-M. Kim, *J. Biomed. Opt.*,  
465 2013, **19**, 051207.
- 466 16 I. L. Gunsolus, M. P. S. Mousavi, K. Hussein, P. Bühlmann and C. L. Haynes,  
467 *Environ. Sci. Technol.*, 2015, **49**, 8078-8086.
- 468 17 G. V. Shelke, C. Lässer, Y. S. Gho and J. Lötvall, *J. Extracell. Vesicles*, 2014, **3**,  
469 24783.